6540.
7. Berlin, K.; Breitmaier, E. *Angew. Chem. Int. Ed. Engl.* **1994**, *33*, 219.
8. Ulman, A.; Manassen, J. *J. Chem. Soc., Perkin Trans. 1*, **1979**, 1066.
9. (a) Broadhurst, M. J.; Grigg, R.; Johnson, A. W. *J. Chem. Soc. (D)*, **1970**, 807. (b) Broadhurst, M. J.; Grigg, R.; Johnson, A. W. *J. Chem. Soc. (D)*, **1969**, 1480. (c) Broadhurst, M. J.; Grigg, R.; Johnson, A. W. *J. Chem. Soc. (C)*, **1969**, 3681.
10. Grazynski, L. L.; Lisowski, J.; Olmstead, M. M.; Balch, A. L. *Inorg. Chem.* **1989**, *28*, 1183.
11. Chmielewski, P. J.; Grazynski, L. L.; Olmstead, M. M.; Balch, A. L. *Chem. Eur. J.* **1997**, *3*, 268.
12. Grazynski, L. L.; Lisowski, J.; Olmstead, M. M.; Balch, A. L. *J. Am. Chem. Soc.* **1987**, *109*, 4428.
13. Lee, C. H.; Lindsey, J. S. *Tetrahedron* **1994**, *50*, 11427.
14. Smith, K. M. In *Porphyrins and Metalloporphyrins*; Smith, K. M., Ed., Elsevier: The Netherlands; 1976; pp 29-58.
15. Lee, C. H.; Park, J. Y.; Oh, K. T.; Ka, J. W. *Bull. Korean Chem. Soc.* **1997**, *18*, 222.
16. Arsenault, G. P.; Bullock, E.; MacDonald, S. F. *J. Am. Chem. Soc.* **1960**, *82*, 4384.

Photodissociation Dynamics of *t*-butyl Hydroperoxide at 280-285 nm

Seung Keun Shin, Chang Hwan Rhee, and Hong Lae Kim*

Department of Chemistry, Kangwon National University, Chuncheon 200-701, Korea
Received November 1, 1997

The phodissociation dynamics of *t*-butyl hydroperoxide at 280-285 nm has been investigated by measuring laser induced fluorescence spectra of the fragment OH. Measured fractions of the available energy distributed among the fragments are f_t=0.56, f_r(OH)=0.044, f_{int}(*t*-BuO)=0.40, and negligible populations of OH are found in vibrationally excited states. By analyzing the Doppler profiles of the spectra of OH, the positive v-J vector correlation has been obtained. From the measured v-J correlation and A" propensity in the two Λ-doublets of OH, it is concluded that the dissociation takes place directly from the repulsive surface induced by the $\sigma^* \leftarrow n$ transition with the fragment OH rotating in the plane perpendicular to the dissociating O-O bond axis.

Introduction

Photochemical reactions are of fundamental importance to study chemical reaction dynamics in detail.[1,2] Since the molecules of interest collide with photons with well-defined momenta, theories are much simpler than those of reactive scattering events and applicable to even moderately large molecules. The processes are governed by an initially prepared state and shape of potential energy surfaces along the reaction coordinate. By examining the dynamics of the process, one can study the shape of the potential energy surfaces in detail and thus electronic structures of the molecules as well.

Studies of photodissociation dynamics in detail require precise measurements of certain physical properties related to the potential energy surfaces. Population and energy distributions among quantum states of the reactants and products are scalar properties from which mechanism of the photodissociation can be deduced. However, in most cases, measuring the energy distribution is not enough to study the detailed dynamics of the process. The transition dipole moment of the parent molecule, recoil velocities and rotational angular momenta of the products are vector properties of the molecule and correlations between these vector properties reveal the detailed dynamics of the photodissociation. In order to measure the angular distribution and speed of the products, a rotatable time-of-flight mass spectrometer has been used.[3] In favorable cases such that the molecules of interest absorb or emit photons of easily accesible spectral region, Doppler resolved absorption or emission spectra provide the translational and internal energy distributions of the fragments. In addition, when linearly polarized lights are used for photolysis and probe, the vector correlations can be measured from the spectra by analyzing the Doppler profiles.[4-6]

The Doppler profiles in polarized absorption and emission spectra of molecules have been thoroughly analyzed by Herschbach and Zare.[7-8] The molecules absorb a photon and are excited when the transition dipole moment μ is preferentially aligned in the laboratory frame parallel to the electric vector, ε_a of the linearly polarized dissociating light. The resulting angular distribution of the photofragments is described by the so-called anisotropy parameter which shows the correlation between μ and the recoil direction of the fragments. When the photofragments are polyatomic molecules, the fragments have rotational angular momenta which have definite relationship with the recoil velocities. Since this v-J correlation is developed when the fragmentation occurs, the v-J correlation may appear even when the angular distribution is isotropic. Correlations of rotation with translational motion have been thoroughly analyzed by Dixon[9] and the anisotropy is defined by a number of bipolar moments of the translational and rotational angular distributions. The Doppler broadened lineshape in the spectra

of the photofragments depends upon rotational alignment, polarization of the photolysis and probe laser lights, excitation-detection geometries, and rotational branch transitions probed. Thus by analyzing the Doppler profiles of the absorption spectra, one can measure the correlations between the vector properties of the fragments.

Photodissociation of $(CH_3)_3COOH$ is one of the good examples of studying the dynamics by applying the Doppler spectroscopic technique. It is particularly interesting to study the effect of alkyl substitution in H_2O_2 on the dynamics, because the symmetry is lower and the substituted group is relatively heavy. $(CH_3)_3COOH$ is dissociated into *t*-butoxy and OH radicals upon irradiation of the UV light. The photodissociation at 248 nm has been studied and slightly negative μ-$v(\beta=-0.2)$ and positive v-J vector correlations at high J have been measured.[10] In the case of H_2O_2 at 266 nm, the negative μ-$v(\beta=-1)$ correlation has been reported.[11] The electronic transition in this energy region is assigned as $\sigma^* \leftarrow n$ that is perpendicular according to simple molecular orbital considerations for both but the relatively heavy *t*-butyl group affects the dynamics of dissociation resulting in the smaller anisotropy parameter. Crim and coworkers have studied the vibration-mediated photodissociation *via* the fifth overtone excitation of the OH stretching vibration. They found large internal excitation in the *t*-butoxy group compared to the direct dissociation from the repulsive surface.[12]

In this experiment, the photodissociation of $(CH_3)_3COOH$ at 280-285 nm has been studied where the fragment OH absorbs *via* the $v=1 \leftarrow 0$, $A \leftarrow X$ transition and emits radiation. The spectra of the fragment OH have been measured by laser induced fluorescence. From the spectra, the energy distribution in the fragments and the *A*-doublet distribution in OH have been measured. Because of the lack of the number of experimental geometries, the complete vector correlations could not be measured but the positive v-J correlation has been deduced by analyzing the Doppler broadened spectra. The dynamics of the dissociation is discussed from the experimental results.

Experiment

The experiment was performed in a flow cell with a conventional pump-probe geometry. The cell was a cube made of stainless steel with two arms in which baffles were placed to minimize scattered light. The cell was evacuated at about 10^{-3} Torr and gaseous $(CH_3)_3COOH$ was continuously flowed at a sample pressure of about 50 mTorr.

The dissociating light was a frequency-doubled output of a dye laser (Lumonics HD 500) which was pumped by the second harmonic of an Nd : YAG laser (Lumonics YM 800). The same laser light probed OH by laser induced fluorescence (LIF) employing the $A \leftarrow X$ transition in the UV region. The pulsewidth was about 8 ns which was measured by a fast photodiode. The photodissociation of the parent molecules and probing the fragments were carried out with the same laser pulse. Thus, we believed that the 50 mTorr sample pressure should provide the nascent product energy distribution. The $1 \leftarrow 0$ transition in OH was excited (280-285 nm) and the total emission was probed without any filter in order to measure the correct intensity distribution. The power of the laser light was kept as low as possible to minimize the scattered radiation, which was in turn discriminated with a gated integrator. The laser power was less than 50 μJ/pulse to avoid saturation as well. The bandwidth of the laser light was 0.08 cm^{-1} in the visible which was measured from the spectra of gaseous I_2 in a static cell at ambient temperature. Since the laser light was horizontally polarized, the pump-probe geometry provided $\varepsilon_d \perp k_p$ where ε_d and k_p were the directions of the electric vector and of propagation of the linearly polarized laser light, respectively. In order to measure the complete vector correlations from the Doppler resolved spectra of OH, more than two different experimental geometries were needed. However, in this experiment, only one geometry could be employed. The detector was placed at a right angle to the laser beam.

The laser induced fluorescence was detected by a PMT (Hamammatsu R212UH) through a collection lense and the detected signal was fed to a boxcar averager. The power of the laser beam was monitored with a photodiode and the fluorescence signal was corrected with respect to the laser power. A signal processor (EG&G 4420) digitized the signal which was stored and processed in a PC.

Results and analyses

Photodissociation dynamics of $(CH_3)_3COOH$ at 280-285 nm has been investigated by measuring rotationally resolved laser induced fluorescence (LIF) spectra of the fragment OH. Since the absorption spectra show continuous and relatively flat absorption in this narrow spectral region, no significant variation of absorptivity and of the resulting dynamics is assumed. In Figure 1, the log of signal intensities from the Q-branch transition ($Q_1(5)$) of OH are plotted as a function of the laser power. The plot shows a straight line of a slope of 1.64, which implies the two photon processes as expected because one photon dissociates $(CH_3)_3COOH$ and another subsequent photon in the same laser pulse absorbed by OH gives rise to the laser induced fluorescence.

A portion of the LIF spectra of the OH products is presented in Figure 2. The rotational transitions in the $v=1 \leftarrow 0$ band of the $A \leftarrow X$ transition are resolved and assigned according to Dieke and Crosswhite.[13] From the measured

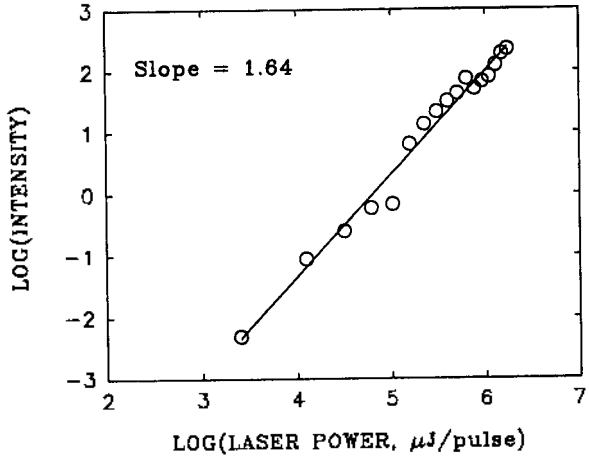

Figure 1. Log of LIF signal intensities measured from the Q-branch rotational transitions as a function of the laser power.

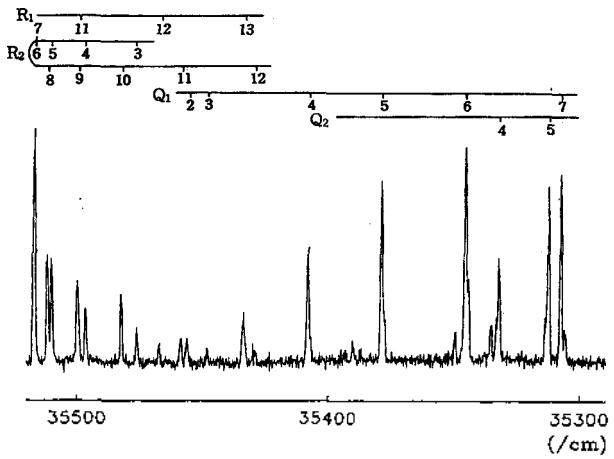

Figure 2. Portion of the LIF spectra of OH produced from the photodissociation of $(CH_3)_3COOH$ at 280-285 nm employing the $1 \leftarrow 0$, $A \leftarrow X$ electronic transition in UV. Rotational assignments are from Ref. 13.

spectra, the rotational population distribution of the OH fragments are obtained from the reported Einstein B coefficients.[14] The rotational population peaks at N=5, 6 and extends to N=13 (Figure 3). From the distribution, the available energy distributed in the product OH rotation is found to be about 1000 cm^{-1} on average. In order to measure vibrational excitation in OH, spectra of the $2 \leftarrow 1$ band region were measured but no appreciable intensities out of noise were observed. Thus, no significant vibrational excitation of OH is concluded in this experiment.

In order to measure the vector correlations and translational energies of the fragments, the Doppler resolved spectra of each rotational transition have been measured. The measured spectra are fitted to the lineshape function[15]

$$I(v)=\int \frac{W(v)}{2v}\,[1+\beta_{eff}P_2(\cos\theta_{e,z})P_2(\cos\theta_{v,z})]\,dv$$

where $W(v)$ is the speed distribution of the fragments, $\theta_{e,z}$ and $\theta_{v,z}$ are angles between the propagation direction of the probe light and the electric vector and the recoil direction, respectively, β_{eff} is the anisotropy parameter composed of the bipolar moments, and $P_2(x)$'s are the second order Legendre Polynomials. The speed distribution represents the internal energy distribution of the corresponding t-BuO radical, which is not measured in this experiment. Thus, the Gaussian distribution with a finite width is used for $W(v)$. Since the experimental geometry in this experiment provides $\theta_{e,z}=\pi/2$ and the Doppler shift, Δv is given by $\Delta v/v_0=v\cos\theta_{v,z}/c$, the lineshape function becomes

$$I(v)=\int \frac{W(v)}{2v}\,[1-\frac{1}{2}\beta_{eff}[\frac{3}{2}(\frac{v-v_0}{v_0})^2(\frac{c}{v})^2-\frac{1}{2}]]\,dv$$

where

$$\beta_{eff}=\frac{b_2\beta_0^2(20)+b_3\beta_0^0(22)+b_4\beta_0^2(22)}{b_0+b_1\beta_0^2(02)}.$$

In the above expression, the bipolar moments $\beta_0^2(02)$, $\beta_0^2(20)$, $\beta_0^0(22)$, $\beta_0^2(22)$ represent the rotational alignment, the translational anisotropy, $\beta_{\mu v}(=2\beta_0^2(20))$, the v-J and the μ-v-J photofragment vector correlations, respectively. The multipliers b's can be calculated from the excitation-detection geometries and the angular momentum coupling factors defined by Dixon,[9] which are obtained for the different rotational branch transitions in this experiment.[16] The measured spectra for the Q, P, R rotational branch transitions for the rotational quantum number N=5-13 are fitted to the above lineshape functions to obtain β_{eff}'s with an average speed and the width of the speed distribution. Typical Doppler resolved spectra with the best fits are presented in Figure 4. The measured average speed for N=5 is 3800± 500 m/s which in turn provides the center-of-mass average translational energy of 12,670 cm^{-1}. From the obtained β_{eff}'s and b's, the individual bipolar moments can be calculated by solving the linear equations. However, since the only one excitation-detection geometry is used in this experiment, number of equations are deficient to obtain all four unkowns. In the previous studies of photodissociation of t-butyl hydroperoxide at 248 and 266 nm, the very small or negligible rotational alignment and the translational anisotropy have been reported.[10] Thus, in this experiment, the v-J and the μ-v-J correlations have only been obtained with the rotational alignment and the translational anisotropy neglected. The obtained v-J correlation, $\beta_0^0(22)$'s are presented for N=5-13 in Figure 5. The measured positive correlation implies that the rotational angular momentum is align-

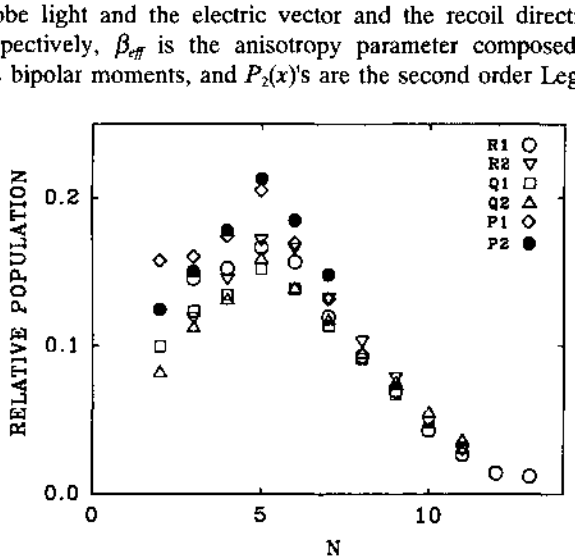

Figure 3. Rotational population distribution of OH obtained from the spectra in Fig. 2.

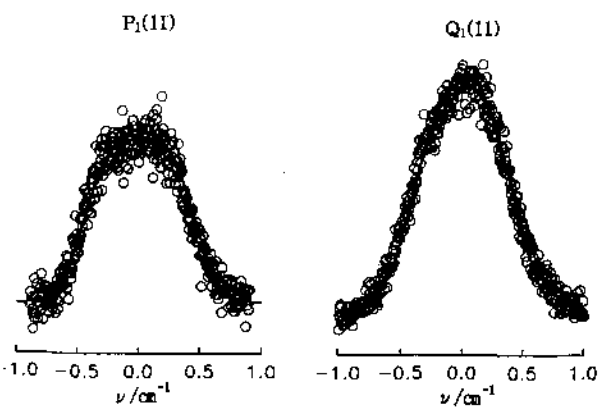

Figure 4. Typical Doppler broadened spectra of OH with the best fits (see text).

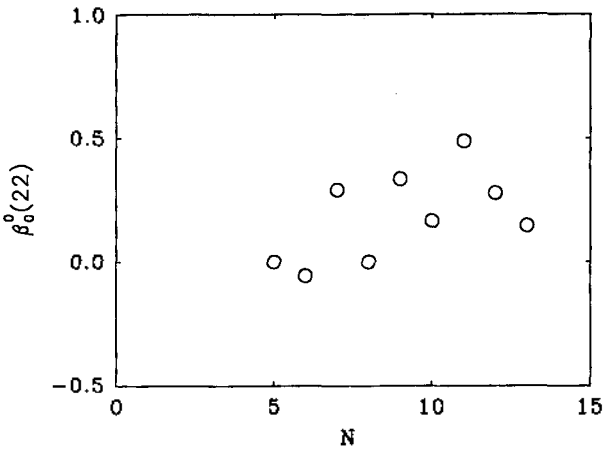

Figure 5. Measured *v*-J correlations obtained from the observed Doppler profiles as a function of the rotational angular momenta N.

ed parallel to the recoil direction.

In Figure 6, the *Λ*-doublet distribution in the OH fragment is presented as a function of the rotational angular momentum J, while the statistical ratio is unity. The measured distribution shows that the A" *Λ*-doublet state is preferentially populated, which suggests that the OH fragment tend to rotate in the plane perpendicular to the dissociating bond axis. Assuming axial dissociation, this again implies that the rotational angular momentum is aligned parallel to the recoil direction.

Discussions

The LIF spectra of the OH fragments from the photodissociation of $(CH_3)_3COOH$ at 280-285 nm have been measured, from which the energy distribution, the *Λ*-doublet distribution in OH and the *v*-J vector correlation of the fragments have been obtained.

The absorption spectra show continuously increasing absorption starting from 320 nm with no maxima in the UV region which has been assigned as the $\sigma^* \leftarrow$ n transition to the ^{1}A excited state for the lowest energy transition. The similar spectra have been obtained for H_2O_2 and CH_3OOH

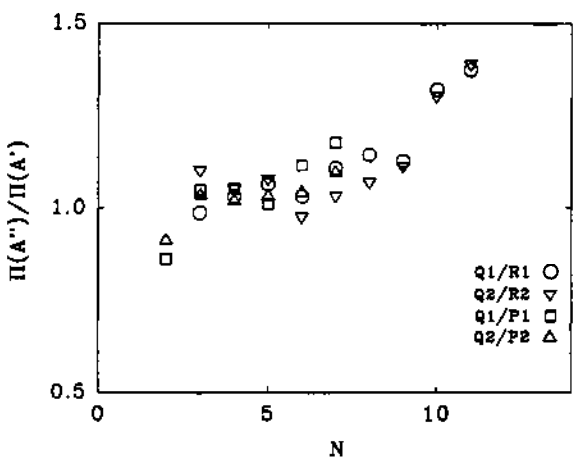

Figure 6. *Λ*-doublet distribution of OH measured from the spectra in Figure 2.

Table 1. Fractions of the available energy distributed in the products produced from the photodissociation of $(CH_3)_3COOH$ at 280-285 nm

E_{av} (cm^{-1})	$<f_t>$	$<f_r(OH)>$	$<f_v(OH)>$	$<f_{int}((CH_3)_3OO)>$
22,802[a]	0.56	0.044	<0.01[b]	0.40
impulsive model	0.58	0.029	0.001	

[a] $E_{av}=h\nu$ (280 nm)+$E_{int}((CH_3)_3COOH)$-$D_0((CH_3)_3CO\text{-}OH)$. [b] Approximated from the noise in the spectra.

and the transition has been found to be perpendicular from the photodissociation of H_2O_2 at 248 ($\beta=-0.86$) and 266 ($\beta=-1$) nm.[11,17] In $(CH_3)_3COOH$, because of the loss of symmetry, the polarization of the transition is less clear, but assuming retention of the $\sigma^* \leftarrow$ n character, the transition dipole moment perpendicular to the O-O axis would be expected. Indeed, the slightly negative translational anisotropies have been measured for the dissociation of $(CH_3)_3$-COOH at 248 nm ($\beta=-0.03\sim-0.27$) indicating the transition is perpendicular. Thus, at 280-285 nm the lowest energy $\sigma^* \leftarrow$ n transition would still be expected.

The available energy distributed among the fragments is the dissociation energy (D_0=14,270 cm^{-1}) subtracted from the photon energy ($h\nu$=35,382 cm^{-1} at 280 nm) and the initial thermal internal energy E_{in} ($(CH_3)_3COOH$) of the parent molecule (1,690 cm^{-1}). Then, the available energy is 22,802 cm^{-1}. The measured fractions of the available energy in the translational and internal degrees of freedom of the fragments are listed in Table 1. The majority of the available energy appears in translation and internal excitation of the *t*-BuO fragment. Impulsive dynamical models, although broadly in agreement with the observed pattern of energy disposal, are unable to predict quantitatively the observed degree of rotational excitation.

Coupling of rotational and electronic orbital angular momenta produces two *Λ*-doublet fine structure states.[18] In diatomic molecules with half-filled electronic orbitals such as OH, an electronic wavefunction of the unpaired electron is, in the limit of high rotation, approximated to the atomic orbital wavefunction which has definite symmetries with respect to the plane of molecular rotation. The symmetric wavefunction represented as a lobe in the plane of rotation is assigned to the A' state among the two *Λ*-doublet components, while the antisymmetric wavefunction as a lobe perpendicular to the plane is assigned to the A" state. These definite parities form rotational selection rules in electronic transitions such as the P- and R-branch transitions should be induced from the A' state and the Q-branch transitions from the A" state. Simple molecular orbital theories predict equal probabilities of forming singly occupied p orbitals in and perpendicular to the OOH plane in the dissociation of H_2O_2 resulting from the $\sigma^* \leftarrow$ n transition and equal population of the two *Λ*-doublet states of the OH fragments has been measured. Since the *t*-Bu group is electron rich compared to H, a nonbonding electron of oxygen in the *t*-BuO is more likely promoted to the σ^* molecular orbital along the O-O axis. In this case, the singly occupied p orbital in the corresponding OH upon dissociation is expected to lie along the dissociation axis. The *Λ*-doublet distribution measured from the P-, R- and Q-branch rotational transitions shows a propensity in the A" state, which implies

that the atomic orbitals for the unpaired electron in the OH fragments formed during the dissociation appear to be aligned perpendicular to the plane of molecular rotation.

The measured v-J correlation, $\beta_0^0(22)$'s are presented in Figure 5. In order to obtain the v-J correlation in this experiment, the rotational alignment and translational anisotropy are neglected because of the lack of number of experimental geometries. Indeed, in the photodissociation of $(CH_3)_3COOH$ at 248 nm and 266 nm,[11] the very small translational anisotropy ($2\beta_0^2(20)=-0.03\sim-0.3$) and the rotational alignment ($\beta_0^2(02)=0.15$) are measured. Even though the same anisotropies measured in the 248 nm photodissociation are used for the calculation, the observed trend in the v-J correlation is not substantially changed. The fraction of photofragments with $v \parallel J$ and $v \perp J$ is related to the v-J correlation, which is given by $f(\parallel)=1/3(1+2\beta_{vJ})$ and $f(\perp)=2/3(1-\beta_{vJ})$, respectively. The measured v-J correlation of 0.5 implies that the 70% of the photofragments are generated with the rotational angular momentum aligned parallel to the recoil velocity. In the *ab initio* calculation[19] of H_2O_2 at the trans planar equilibrium configuration, the dihedral angle, Φ is predicted to be 120° and the barrier for the corresponding *cis-trans* conformational change is about 386 cm^{-1}. The alkyl substitution slightly opens the dihedral angle (Φ=126°) and greatly reduces the barrier (~80 cm^{-1}) for CH_3OOH. Assuming the same trend for the *t*-Bu substitution, even the smaller barrier height is expected which is much less than the zero point energy of the OH torsional motion. Thus, the wide angle torsional motion of OH in $(CH_3)_3COOH$ (while the heavy *t*-BuO group remains essentially fixed in space) is likely transformed into the rotational motion of the OH fragment upon dissociation. In this case, the rotational angular momentum of the OH fragment is likely to be aligned parallel to the recoil velocity along the dissociating O-O bond. The positive v-J correlation and the A'' Λ-doublet propensity measured in this experiement indicate the above fact that implies the OH torsional motion plays an important role for the fragment OH rotation in the photodissociation of $(CH_3)_3COOH$.

In summary, the photodissociation of $(CH_3)_3COOH$ at 280-285 nm starts from the lowest ^1A excited state induced from the $\sigma^* \leftarrow n$ transition. The dissociation is fast and directly generates the OH fragments rotating in the plane perpendicular to the dissociating O-O bond axis (out-of-plane dissociation). The rotational motion of the fragment OH mainly originates from the parent wide angle torsional motion of OH while the heavy *t*-BuO group remains fixed in space.

Acknowledgments. This work has been supported by the Korea Research Foundation and the Ministry of Education of Korea.

References

1. Singer, S. J.; Freed, K. F.; Band, Y. B. *Adv. Chem. Phys.* **1985**, *61*, 1
2. Schinke, R. *Photodissociation Dynamics*; Cambridge University Press: 1993
3. Riley, S. J.; Wilson, K. R. *Faraday Discuss. Chem. Soc.* **1972**, *53*, 132
4. Hall, G. E.; Houston, P. L. *Ann. Rev. Phys. Chem.* **1989**, *40*, 375.
5. Houston, P. L. *J. Phys. Chem.* **1987**, *91*, 5388.
6. Kim, H. L.; Wickramaaratchi, M. A.; Zheng, X.; Hall, G. E. *J. Chem. Phys.* **1994**, *101*, 2033.
7. Zare, R. N.; Herschbach, D. R. *Proc. IEEE* **1963**, *51*, 173.
8. Greene, G. H.; Zare, R. N. *Ann. Rev. Phys. Chem.* **1982**, *33*, 119.
9. Dixon, R. N. *J. Chem. Phys.* **1986**, *85*, 1866.
10. August, J.; Brouard, M.; Docker, M. P.; Milne, C. J.; Simons, J. P.; Lavi, R.; Rosenwaks, S.; Schwartz-Lavi, D. *J. Phys. Chem.* **1988**, *92*, 5485.
11. Gericke, K-H.; Klee, S.; Comes, F. J.; Dixon, R. N. *J. Chem. Phys.* **1986**, *85*, 4463.
12. Likar, M. D.; Baggott, J. E.; Sinha, A.; Ticich, T. M.; Vander Wal, R. L.; Crim, F. F. *Faraday Trans., J. Chem. Soc.* **1988**, *84*, 1483.
13. Dieke, G. H.; Crosswhite, H. M. *J. Quant. Spectrosc. Radiat. Transfer* **1962**, *2*, 97.
14. Chidsey, I. L.; Crosley, D. R. *J. Quant. Spectrosc. Radiat. Transfer* **1980**, *23*, 187.
15. Ashfold, M. N. R.; Baggott, J. E. (Ed.) *Molecular Photodissociation Dynamics*; Royal Society of Chemistry: London, 1987.
16. Baek, S. J.; Park, C. R.; Kim, H. L. *J. Photochem. Photobiol. A* **1997**, *104*, 13.
17. August, J.; Brouard, M.; Docker, M. P.; Hodgson, A.; Milne, C. J.; Simons, J. P. *Ber. Bunsenges. Phys. Chem.* **1988**, *92*, 264.
18. Hanazaki, I. *Chem. Phys. Lett.* **1993**, *201*, 301.
19. Bair, R. A.; Goddard III, W. A. *J. Am. Chem. Soc.* **1982**, *104*, 2719.